Physical Layer Network Coding Using Gaussian Waveforms: A Link Level Performance Analysis

Matthias Woltering, Dirk Wübben, and Armin Dekorsy
University of Bremen, Bremen, Germany
Email: {woltering, wuebben, dekorsy}@ant.uni-bremen.de

Stephan Schedler, and Volker Kühn
University of Rostock, Rostock, Germany
Email: {stephan.schedler, volker.kuehn}@uni-rostock.de

***Abstract*—Using general waveforms has recently gained omnipresent attention for robustness in systems under practical constraints. In this paper, two way relaying networks using physical layer network coding utilizing a multicarrier scheme with Gaussian waveforms are analyzed. This combination is introduced to be more robust against the impact of carrier frequency offsets and timing offsets. In two way relaying a multiple access phase is applied, where both users transmit their messages simultaneously on the same resources to an assisting relay. Here, a superposition of both signals containing the influence of the individual channels is received. The additional interference introduced by the non-orthogonal Gaussian filter is treated by a linear equalizer. To reduce complexity the equalizer is simplified to treat adjacent symbols in the time-frequency grid, only. To evaluate the overall performance of the introduced equalizer, different decoding strategies are analyzed by means of a link level simulations.**

***Index Terms*—generalized FDM, linear MMSE equalizer, physical-layer network coding, two way relay channel, Link level simulation.**

I. Introduction

Modern communication systems have evolved to networks supporting an increasing number of services. A key technology for future communication systems is the principle of cooperative communication. It offers transmission techniques to enhance the coverage for applications with required Quality of Service (QoS) constraints [1]–[3]. Beside cooperation among sources and destinations, the utilization of relay stations has gained significant interest [3], [4]. Intermediate relay nodes can reduce the path loss significantly and offer spatial diversity. In [5]–[8] the two way relay channel (TWRC) with physical-layer network coding (PLNC) is introduced, where data of two users is exchanged over an assisting relay as shown in Fig. 1. In the Multiple Access (MA) phase both users transmit their data simultaneously on the same resources to the relay and in a following broadcast (BC) phase the relay transmits a network coded signal back to both users. As the users are aware of their own message, they are able to extract the desired message of the other user from the network coded message.

As both nodes are transmitting simultaneously to the relay, a major implementation challenge is the removal of inherent time and frequency offsets due to different oscillators or dispersive channel realizations. Since Orthogonal Frequency Division Multiplexing (OFDM) is widely used as multicarrier transmission scheme in current mobile transmission standards, the combination of OFDM and PLNC has been proposed in [9]–[15]. However, in [16] it was shown that OFDM in TWRCs suffers from carrier frequency offset causing Inter-Carrier Interference (ICI). Much research has been done to improve the robustness of multicarrier systems regarding these effects.

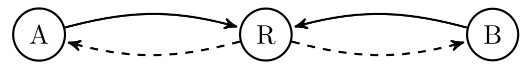

Fig. 1. A TWRC with MA phase (solid lines) and BC phase (dashed lines).

Besides OFDM many multicarrier schemes are known, where alternative transmit and receive filters are used instead of the rectangular one in OFDM. In [17] subcarrier-wise filtering is considered named Offset-QAM/Filter Bank Multi-Carrier (OQAM/FBMC). Here, well-localized filters are used to generate an orthogonal transmit scheme. Another scheme is universal filtered multicarrier (UFMC), which is a subblock-based filtered OFDM system introduced in [18]. More generalized schemes, which utilize non-orthogonal multicarrier transmission are given in [19], [20]. In [19] an introduction to generalized FDM (GFDM) is given, whereas [20] deals with a block-based realization, similar to OFDM. An overview of non-orthogonal waveforms in mobile applications is given in [21].

In this paper, a Gaussian prototype filter in combination with GFDM and PLNC is used. Contrary to an OFDM system, which is in the ideal case perfectly orthogonal, a Gaussian prototype filter introduces inter-symbol interference (ISI) and ICI even in a synchronized system. However, a Gaussian prototype filter decays fast such that interference is mainly limited to adjacent time-frequency points. Furthermore, it has the same shape in time and frequency and it is optimally concentrated [17], [22]. One approach to treat the interference is a linear Minimum Mean Square Error (MMSE) equalizer. This paper focuses on the implementation of PLNC and GFDM with Gaussian waveforms in a link level simulation, including the impact of practical implementation constraints.

The paper is organized as follows. In Section II, a PLNC system model is given using general filters. First, the signal which is received at the relay is derived, then a linear equalizer with respect to MMSE criterion is introduced. Furthermore, the decoding and detection schemes are briefly introduced. In Section III simulation results are presented and Section IV concludes the paper.

Notations: In this paper, lower case bold characters are used to denote vectors, upper case bold characters denote matrices. $(\cdot)^T$ denotes the transpose of a vector, $(\cdot)^*$ is the conjugate

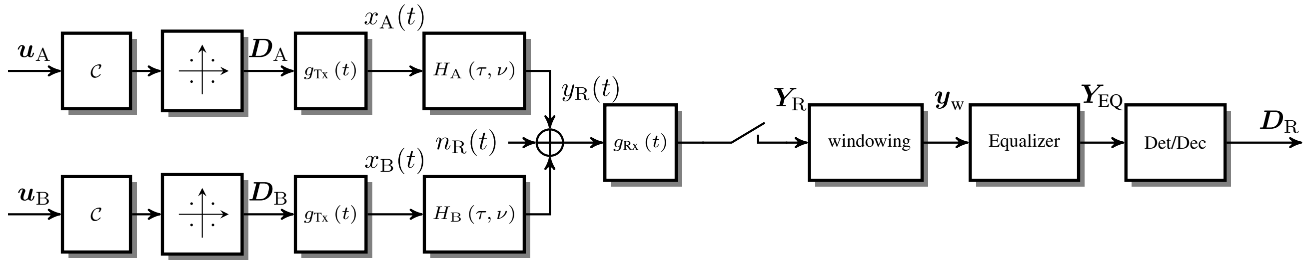

Fig. 2. Block diagram of the MA phase of a PLNC system with Generalized FDM (GFDM)

complex, $(\cdot)^H$ is the conjugate transposed and $p(\cdot)$ is a Probability Density Function (PDF).

II. System Description

A. Relay Receive signal

As depicted in Fig. 2, $\boldsymbol{u}_A$ and $\boldsymbol{u}_B$ denote binary sequences of user A and user B which get encoded by a linear $\mathcal{C}$ code with code rate R_C. The coded binary sequences $\boldsymbol{c}_A = \mathcal{C}(\boldsymbol{u}_A)$ and $\boldsymbol{c}_B = \mathcal{C}(\boldsymbol{u}_B)$ are modulated with a M-QAM to symbol sequences. These sequences are mapped to matrices $\boldsymbol{D}_A$ and $\boldsymbol{D}_B$, where each element $d_A^{(k,\ell)}$ and $d_B^{(k,\ell)}$ is related to one point in a time-frequency grid (k,ℓ). The dimension are $N_K \times N_L$, where N_K and N_L give the number of symbols per frame in frequency and time dimension, respectively. Each symbol is shifted on the corresponding k^{th} subcarrier in the ℓ^{th} time slot by the transmit filter $g_{Tx}^{(k,\ell)}(t)$:

$$g_{Tx}^{(k,\ell)}(t) = g(t-\ell T)\, e^{j2\pi kFt} \quad , \tag{1}$$

where t is continuous time variable, F denotes subcarrier spacing and T is symbol spacing. The matched filter at the receiver, corresponding to (1), is given by

$$g_{Rx}^{(k',\ell')}(t) = g^*(-t-\ell' T) \cdot e^{-j2\pi(k'F)(-t)} \quad . \tag{2}$$

Both transmit signals will pass individual channels $H(\tau,\nu)$. The delay-Doppler function is the Fourier transform of $H(\tau,\nu) \bullet\!\!-\!\!\circ\, h(\tau,t)$ regarding t and given by

$$H(\tau,\nu) = \sum_{\iota=0}^{N_h-1} h_\iota \delta(\tau-\tau_\iota-\Delta\tau)\delta(\nu-\nu_\iota-\Delta\nu) \quad , \tag{3}$$

where $h_\iota, \tau_\iota, \nu_\iota$ are the complex channel coefficient, time delay and Doppler shift of tap $\iota = 0,\dots,N_h-1$. Additionally carrier frequency offset (CFO) $\Delta\nu$ and timing offset (TO) $\Delta\tau$ are introduced in (3), which occur individually on each user link. The assisting relay receives the superposition of both signals and additive white Gaussian noise (AWGN) with $n_R(t) \sim \mathcal{CN}(0,\sigma_n^2)$. And the received signal after matched filtering and sampling at the relay on the time and frequency point (k',ℓ') is given by [23]

$$y_R^{(k',\ell')} = \sum_{k=0}^{N_K-1}\sum_{\ell=0}^{N_L-1} d_A^{(k,\ell)} v_A^{(k,\ell,k',\ell')} + \sum_{k=0}^{N_K-1}\sum_{\ell=0}^{N_L-1} d_B^{(k,\ell)} v_B^{(k,\ell,k',\ell')} + \widetilde{n}_R^{(k',\ell')} \quad , \tag{4}$$

where $\widetilde{n}_R^{(k',\ell')}$ is the filtered noise at the relay. The coefficients $v_i^{(k,\ell,k',\ell')}$ with $i \in \{A,B\}$ defined in (5) on the next page, combine the impact of the channel $H(\tau,\nu)$ as well as the transmit and receive filter for the corresponding transmit signals $d_A^{(k,\ell)}$ and $d_B^{(k,\ell)}$ on the receive signal $y_R^{(k',\ell')}$. The auto-ambiguity function used in (5) is defined like [19]

$$A(\tau,\nu) = \int g\left(t+\frac{\tau}{2}\right) g^*\left(t-\frac{\tau}{2}\right) e^{-j2\pi\nu t} dt \quad , \tag{6}$$

describes the influences on a specific time and frequency point given a filter $g(\cdot)$. It is depicted for a Gaussian as well as for a rectangular filter in Fig. 3.

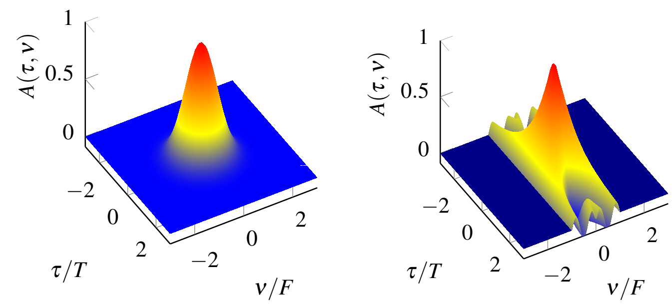

(a) Gaussian prototype filter (b) Rectangular prototype filter

Fig. 3. Ambiguity function of the (a) isotropic Gaussian and a (b) rectangular filter, respectively

Hence, the sampled receive signal after matched filtering at the relay can also be given by matrix notation:

$$\boldsymbol{y}_R = \boldsymbol{V}_A \cdot \boldsymbol{d}_A + \boldsymbol{V}_B \cdot \boldsymbol{d}_B + \boldsymbol{n}_R \quad . \tag{7}$$

Here, the operator vec$\{\cdot\}$ which stack the columns of a matrix to a vector and it is used to generate the symbol vectors $\boldsymbol{d}_A = \text{vec}\{\boldsymbol{D}_A\}$ and $\boldsymbol{d}_B = \text{vec}\{\boldsymbol{D}_B\}$. The receive signal $\boldsymbol{y}_R$ can also be interpreted as a stacked vector $\boldsymbol{y}_R = \text{vec}\{\boldsymbol{Y}_R\}$.

$$v_i^{(k,\ell,k',\ell')} = \iint H_i(\tau,\nu)\, e^{-2j\pi\left(kF\tau+\left(F\left(k'-k\right)-\nu\right)\left(\frac{1}{2}\left(\left(\ell'+\ell\right)T+\tau\right)\right)\right)} \cdot A^*\left(T\left(\ell-\ell'\right)+\tau, F\left(k-k'\right)+\nu\right) d\nu d\tau \tag{5}$$

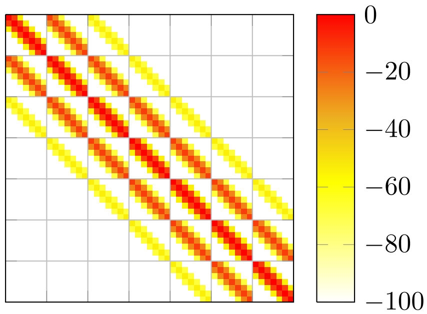

Fig. 4. Absolute values of the elements in matrix $\boldsymbol{V}_i$ for one user in logarithmic scale

Exemplary, Fig. 4 depicts the absolute values of matrix $\boldsymbol{V}$ for a Gaussian transmit filter, a simple AWGN channel with $H(\tau,\nu)=\delta(\tau)\delta(\nu)$ and frames with symbols on $N_\mathrm{L}\times N_\mathrm{K} = 7\times 7$ time frequency grid. Due to the small influence to adjacent time-frequency points, matrix $\boldsymbol{V}$ is sparse for well localized filters as also indicated by the ambiguity function in Fig. 3, which motivates that only considering some neighbors in the equalizer could be sufficient.

B. Equalizer

The goal at the equalizer output is to reduce the influence of the interference (ISI and ICI) introduced by the channel and the filters and provide a signal which is only dependent on the desired signals. As described in [24], the influence of non-orthogonal filters and doubly dispersive channels are highly complex and the optimal sequence estimator is a Viterbi algorithm working on a state diagram including all possible states in time and frequency. Here, we focus on a linear equalizer taking only adjacent symbols in time-frequency grid into account. The restriction to a small number of neighboring symbols is motivated by the auto-ambiguity function of the Gaussian prototype filter depicted in Fig. 3(a). Contrary to the ambiguity function of a rectangular prototype filter in Fig 3(b), the Gaussian waveform is well concentrated in time and frequency, i.e. the interference terms are limited to adjacent time-frequency points. As the interference only occupy some neighbors, the input of the equalizer could be reduced to a vector with smaller size. A window matrix operator as

$$\omega_{(k',\ell')}^{N_\mathrm{N}}\{\boldsymbol{A}\} = \mathrm{vec}\{[\boldsymbol{A}]_{(k'-N_\mathrm{N}:k'+N_\mathrm{N})(\ell'-N_\mathrm{N}:\ell'+N_\mathrm{N})}\} \tag{8}$$

which selects a rectangular window out of a matrix $\boldsymbol{A}$ depending on a number of neighbors N_N around (k',ℓ') in each direction. Without loss of generality, we assume here that the window is squared, the operator can easily extend to window that use different neighbors in frequency and time direction Hence, by using this operator the equalizer input for a specific time-frequency point (k',ℓ') at the relay uses a windowed received signal

$$\boldsymbol{y}_\mathrm{w}^{(k',\ell')} = \omega_{(k',\ell')}^{(N_\mathrm{N})}\{\boldsymbol{Y}_\mathrm{R}\} \quad , \tag{9}$$

which is approximated from $\boldsymbol{Y}_\mathrm{R}$. It considering only some neighbors and has the size $(2N_\mathrm{N}+1)^2\times 1$. This windowed receive signal in (9) can be written as

$$\boldsymbol{y}_\mathrm{w}^{(k',\ell')} = \tilde{\boldsymbol{V}}_\mathrm{A}\cdot\boldsymbol{d}_\mathrm{A} + \tilde{\boldsymbol{V}}_\mathrm{B}\cdot\boldsymbol{d}_\mathrm{B} + \boldsymbol{n}_\mathrm{w,R}^{(k',\ell')} \quad . \tag{10}$$

$\tilde{\boldsymbol{V}}_\mathrm{A}$ and $\tilde{\boldsymbol{V}}_\mathrm{B}$ are matrices which have reduced size corresponding to (8) and they contain the corresponding coefficients given by (5) and $\boldsymbol{n}_\mathrm{w,R}^{(k',\ell')}$ is the windowed noise vector. The size of these matrices is $(2N_\mathrm{N}+1)^2\times(N_\mathrm{L}\cdot N_\mathrm{K})$. The output of a linear equalizer $\boldsymbol{z}^{(k',\ell')}$ is given by

$$y_\mathrm{EQ}^{(k',\ell')} = \left(\boldsymbol{z}^{(k',\ell')}\right)^T \boldsymbol{y}_\mathrm{w}^{(k',\ell')} \quad . \tag{11}$$

Note that the output of the equalizer $y_\mathrm{EQ}^{(k',\ell')}$ are elements of a matrix denoted as $\boldsymbol{Y}_\mathrm{EQ}$.

The equalizer coefficients to estimate the superposition $d_\mathrm{A}^{(k',\ell')} = d_\mathrm{B}^{(k',\ell')}$ of the data are determined assuming MMSE criterion, by solving optimization problem

$$\boldsymbol{z}_\mathrm{MMSE}^{(k',\ell')} = \underset{\boldsymbol{z}^{(k',\ell')}}{\arg\min}\ \mathrm{E}\left\{\left|y_\mathrm{EQ}^{(k',\ell')} - \left(d_\mathrm{A}^{(k',\ell')} + d_\mathrm{B}^{(k',\ell')}\right)\right|^2\right\} . \tag{12}$$

The solution is given by [25]

$$\left(\boldsymbol{z}_\mathrm{MMSE}^{(k',\ell')}\right)^\mathrm{T} = \boldsymbol{e}^\mathrm{T}\left(\tilde{\boldsymbol{V}}_A^H + \tilde{\boldsymbol{V}}_B^H\right)\left(\tilde{\boldsymbol{V}}_A\,\tilde{\boldsymbol{V}}_A^H + \tilde{\boldsymbol{V}}_B\,\tilde{\boldsymbol{V}}_B^H + \frac{\sigma_\mathrm{n}^2}{\sigma_\mathrm{S}^2}\boldsymbol{I}\right)^{-1}, \tag{13}$$

where vector $\boldsymbol{e}^\mathrm{T} = [0,\cdots,0,1,0,\cdots,0]$ selects the row that corresponds to the desired symbol (k',ℓ').

Considering a smaller number of neighbors reduces the complexity. The impact of the interference is directly connected to the window size. If N_N adjacent neighbors are considered by the equalizer, the interference caused by the $(2N_\mathrm{N}+1)^2$ neighbors around symbol (k',ℓ') will be considered. The interference of time-frequency points that are more than $N_\mathrm{N}+1$ symbols away, is not considered by the equalizer. The larger N_N, the smaller the impact of the residual interference. For a frame size of $N_\mathrm{Fr} = N_\mathrm{L}\cdot N_\mathrm{K}$ symbols, the complexity of a full inversion in (13) is of order $\mathcal{Q}_\mathrm{full}\sim\mathcal{O}(N_\mathrm{Fr}^3)$, whereas a reduced equalizer requires N_Fr inversions of a matrix with size $(2N_\mathrm{N}+1)^2$ which is of order $\mathcal{Q}_\mathrm{reduced}\sim\mathcal{O}(N_\mathrm{Fr}\cdot((2N_\mathrm{N}+1)^2)^3)$. As shown in Fig. 5 considering only some neighbors reduces the complexity only, if N_N is small. For a frame of size $N_\mathrm{Fr} = 320$ elements, complexity can be reduced only if $N_\mathrm{N}\leq 3$.

$$p\left(y_{\mathrm{EQ}} \mid d_{\mathrm{AB}}\right) \approx \frac{1}{\pi\left(\sigma_{\mathrm{n,EQ}}^2+\sigma_{\mathrm{I}}^2\right)} \exp\left(-\frac{\left\|y_{\mathrm{R}}-v_{\mathrm{A}} d_{\mathrm{A}}-v_{\mathrm{B}} d_{\mathrm{B}}\right\|^2}{\sigma_{\mathrm{n,EQ}}^2+\sigma_{\mathrm{I}}^2}\right) \tag{14}$$

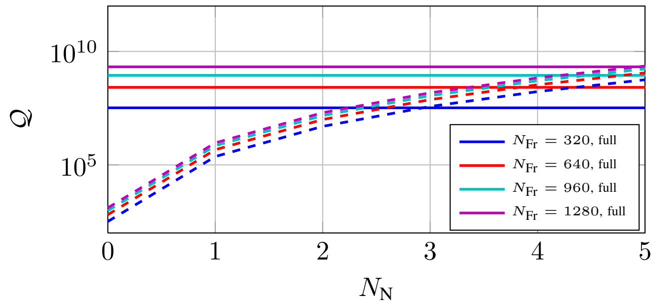

Fig. 5. Complexity of a full inversion (—), and inversion of reduced size matrix (- -)

C. Detection and Decoding

The goal of the detection and decoding block is to generate a relay codeword $\boldsymbol{c}_{\mathrm{R}}$ which is mapped to a symbol matrix $\boldsymbol{D}_{\mathrm{R}}$ containing all symbols to transmit a network coded signal back to the user A and B in the BC phase. The task at the detector and decoding block is to maintain this network coded signal $\boldsymbol{c}_{\mathrm{R}}$ from the equalizer signal $y_{\mathrm{EQ}}^{(k',\ell')}$. In [25], [26] different decoding and detection schemes for PLNC are analyzed, which uses different estimation schemes. In general, all detection schemes share the same a-posteriori probability (APP) calculation, where the input signal of the decoding stage is calculated.

1) Seperate Channel Decoding (SCD): First, SCD is introduced [11], where the relay uses two seperate decoders to estimate each individual message $\hat{\boldsymbol{u}}_{\mathrm{A}}$ and $\hat{\boldsymbol{u}}_{\mathrm{B}}$, separately. At one decoder the signal of the other user is treated as interference completely. The input signal of each decoder A is based on the Log-Likelihood Ratios (LLRs) $L(\boldsymbol{c}_{\mathrm{A}})$ and of decoder B on $L(\boldsymbol{c}_{\mathrm{B}})$. The LLRs are generated out of the APPs, i.e. the LLR of a single codebit is calculated as

$$L(c_{\mathrm{A}}) = \log \frac{\Pr\left\{c_{\mathrm{A}}=0|y_{\mathrm{R}}\right\}}{\Pr\left\{c_{\mathrm{A}}=1|y_{\mathrm{R}}\right\}} = \log \frac{\sum_{\mathcal{D}_{\mathrm{S,A}}^{0}} p\left(y_{\mathrm{R}}|d_{\mathrm{AB}}\right)}{\sum_{\mathcal{D}_{\mathrm{S,A}}^{1}} p\left(y_{\mathrm{R}}|d_{\mathrm{AB}}\right)} \quad , \tag{15}$$

where $\mathcal{D}_{\mathrm{S,A}}^{\kappa}$ is the set containing all symbol pairs $d_{\mathrm{AB}} = (d_{\mathrm{A}}, d_{\mathrm{B}})$ with involved bit $c_{\mathrm{A}} = \kappa$. The same calculations are done to get the LLRs codebits $L(\boldsymbol{c}_{\mathrm{B}})$. After estimating, the relay performs the XOR combination of the estimated user data to generate the relay codeword $\boldsymbol{c}_{\mathrm{R}} = \mathcal{C}(\hat{\boldsymbol{u}}_{\mathrm{A}}) \oplus \mathcal{C}(\hat{\boldsymbol{u}}_{\mathrm{B}})$.

2) Joint Channel decoding and physical-layer Network coding (JCNC): JCNC is a approach that jointly estimates the XORed codeword $\boldsymbol{c}_{\mathrm{R}}$ [5] based on the LLR $L(c_{\mathrm{A}\oplus\mathrm{B}})$, i.e. the LLR of a single codebit is calculated as

$$L(c_{\mathrm{A}\oplus\mathrm{B}}) = \log \frac{\Pr\left\{c_{\mathrm{A}\oplus\mathrm{B}}=0|y_{\mathrm{R}}\right\}}{\Pr\left\{c_{\mathrm{A}\oplus\mathrm{B}}=1|y_{\mathrm{R}}\right\}} = \log \frac{\sum_{\mathcal{D}_{\mathrm{J}}^{0}} p\left(y_{\mathrm{R}}|d_{\mathrm{AB}}\right)}{\sum_{\mathcal{D}_{\mathrm{J}}^{1}} p\left(y_{\mathrm{R}}|d_{\mathrm{AB}}\right)} \quad , \tag{16}$$

where $\mathcal{D}_{\mathrm{J}}^{\kappa}$ is the set containing all symbol pairs $d_{\mathrm{AB}} = (d_{\mathrm{A}}, d_{\mathrm{B}})$ with involved bit $c_{\mathrm{A}\oplus\mathrm{B}} = \kappa$. Here the decoding is done by using only one decoder, which directly detects the codeword $\boldsymbol{c}_{\mathrm{R}}$.

3) Generalized Joint Channel decoding and physical-layer Network coding (G-JCNC): The G-JCNC scheme perfroms joint decoding of both channel codes by directly feeding the symbol-APPs to a non-binary channel decoder in order to fully exploit the coding gain [8].

4) APP calculation: As described above each scheme needs to calculate the APPs. At the output of the equalizer in (11) the signal can be separated into desired signal, interference signal and noise signal given by

$$\begin{aligned} y_{\mathrm{EQ}}^{(k',\ell')} &= \boldsymbol{v}_{\mathrm{EQ,A}}^{\mathrm{T}} \boldsymbol{d}_{\mathrm{A}} + \boldsymbol{v}_{\mathrm{Eq,B}}^{\mathrm{T}} \boldsymbol{d}_{\mathrm{B}} + \left(\boldsymbol{z}^{(k',\ell')}\right)^{T} \boldsymbol{n}_{\mathrm{w,R}}^{(k',\ell')} \\ &= v_{\mathrm{S,A}} d_{\mathrm{A}}^{(k',\ell')} + v_{\mathrm{S,B}} d_{\mathrm{B}}^{(k',\ell')} + y_{\mathrm{I}}^{(k',\ell')} + n_{\mathrm{EQ,R}}^{(k',\ell')} \quad , \end{aligned} \tag{17}$$

where $\boldsymbol{v}_{\mathrm{EQ,A}}^{\mathrm{T}} = \left(\boldsymbol{z}^{(k',\ell')}\right)^{T} \cdot \tilde{\boldsymbol{V}}_{\mathrm{A}}$ is the overall effective channel vector for user A including the equalizer, waveforms and the channel. For user B coefficient vector $\boldsymbol{v}_{\mathrm{EQ,B}}^{\mathrm{T}}$ are defined in the same way. The elements $v_{\mathrm{S,A}} = v_{\mathrm{EQ,A}}^{(k',\ell',k',\ell')}$ and $v_{\mathrm{S,B}} = v_{\mathrm{EQ,B}}^{(k',\ell',k',\ell')}$ are scalar channel coefficients for the desired signal. The sum of interference terms $y_{\mathrm{I}}^{(k',\ell')}$ of both users is given by

$$y_{\mathrm{I}}^{(k',\ell')} = \sum_{i} \sum_{\substack{k \\ (k,\ell)\neq(k',\ell')}} \sum_{\ell} v_{\mathrm{EQ},i}^{(k,\ell,k',\ell')} d_{i}^{(k,\ell)} \quad . \tag{18}$$

The noise term reads

$$n_{\mathrm{EQ,R}}^{(k',\ell')} = \left(\boldsymbol{z}^{(k',\ell')}\right)^{T} \boldsymbol{n}_{\mathrm{w,R}}^{(k',\ell')} \quad , \tag{19}$$

with $n_{\mathrm{EQ,R}}^{(k',\ell')} \sim \mathcal{CN}(0, \sigma_{\mathrm{n,EQ}}^2)$. For APP computation the interference terms are assumed to be complex normal distributed with $y_{\mathrm{I}}^{(k',\ell')} \sim \mathcal{CN}(0, \sigma_{\mathrm{I}}^2)$. Then the calculation of the APPs can be approximated by (14), omitting the time frequency index for brevity.

III. Simulation

A multicarrier system with binary phase-shift keying (BPSK) modulation is considered. For simulation a Raleigh fading channel with exponentially decreasing power delay profile and equally distributed Doppler shifts is used. Each frame is encoded by an Low Density Parity Check (LDPC) code with code rate $R_{\mathrm{C}} = 0.3$, which is matched on a frame with the size of $N_{\mathrm{K}} = 16$ subcarriers and $N_{\mathrm{L}} = 10$ time symbols, so that in total 160 symbols are transmitted per frame. To generate transmit signals $x_{\mathrm{A}}(t)$ and $x_{\mathrm{B}}(t)$ given in

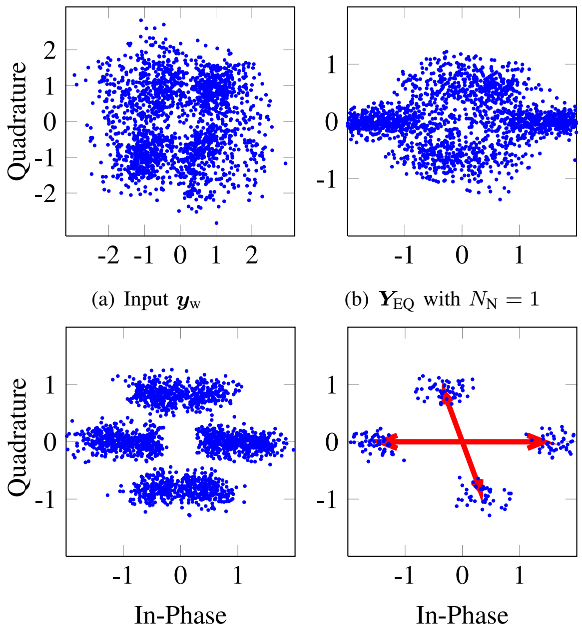

(a) Input $\boldsymbol{y}_{\mathrm{w}}$

(b) $\boldsymbol{Y}_{\mathrm{EQ}}$ with $N_{\mathrm{N}}=1$

(c) $\boldsymbol{Y}_{\mathrm{EQ}}$ with $N_{\mathrm{N}}=2$

(d) $\boldsymbol{y}_{\mathrm{EQ}}^{(k'=1,\ldots,N_{\mathrm{K}}-1,\ell'=1)}$ with possible constellations depicted with red arrows, and $N_{\mathrm{N}}=1$

Fig. 6. Equalizer signals of a whole frame. (a) equalizer input given by (7), (b) and (c) equalizer output in (17), and (d) output signal at one specific time instance

Fig. 2, a polyphase based network [22] is used, and transmit and receive filters are sampled by $T_{\mathrm{s}}=\frac{T}{o \cdot N_{\mathrm{K}}}$, where o is the factor as a multiple of the number of subcarriers. In the following results the oversampling is set to $o=8$, where an overall oversampling of 128 is generated to approximate the Gaussian waveform to a quasi analog system in the simulation.

First, the impact of the equalizer is exemplary analyzed using fixed channels given in Table I. All elements of the input signal of the equalizer $\boldsymbol{y}_{\mathrm{w}}$ are shown in a scatterplot in Fig. 6(a). It includes the impact of transmit filters as well as the influence of the frequency selective channels. Fig. 6(b) and Fig. 6(c) illustrates the equalizer output $\boldsymbol{Y}_{\mathrm{EQ}}$ of all symbols of one frame using $N_{\mathrm{N}}=1$ or 2 neighbors, respectively. In the ideal case (no noise, no interference) four discrete constellations points are expected due to (17), where the impact of the interference term should be small. Note that the signals show still a residual impact of the interference, Fig. 6(c) reduces this terms to smaller cluster of points than Fig. 6(b). In Fig. 6(d) shows the output signal for $N_{\mathrm{N}}=1$ on a time instance $\ell'=1$. Here, the red arrows depict the hypotheses $\upsilon_{\mathrm{S,A}} d_{\mathrm{A}}^{(k',\ell')}+\upsilon_{\mathrm{S,B}} d_{\mathrm{B}}^{(k',\ell')}$ without presence of interference and noise, which are used to calculate the APPs in (14). The cluster of points are still well located to the given hypotheses, choosing one neighbor $N_{\mathrm{N}}=1$.

Regarding bit error rate (BER) performance measurements general channels are introduced, where a randomly chosen $H(\tau,\nu)$ is used. The maximum delay is restricted to $\tau_{\max}=0.08$T and maximum Doppler shift to $\nu_{\max}=0.08$F.

TABLE I
CHANNEL REALIZATION USED IN FIG. 6

ι	$h_{\mathrm{A},\iota}$	$h_{\mathrm{B},\iota}$	$\tau_\iota/(T_s/o)$	ν_ι
0	$-0.9111+0.1514j$	$0.0204+0.9703j$	0	0
1	$0.2560+0.2363j$	$-0.0305+0.2272j$	1	0
2	$-0.1210-0.0840j$	$-0.0678-0.0005j$	2	0
3	$-0.0427+0.0437j$	$-0.0127+0.0249j$	3	0
4	$0.0104-0.0062j$	$0.0091-0.0109j$	4	0
5	$0.0011-0.0045j$	$-0.0001-0.0031j$	5	0

Fig. 7 shows the overall performance of the different schemes with a Gaussian transmit and receive filter considering an equalizer using the reduced matrices $\tilde{\boldsymbol{V}}_i$ with different numbers of neighbors N_{N} in comparison to the use of the full matrix $\boldsymbol{V}_i$. Obviously, the detection/decoding scheme G-JCNC outperforms the other both schemes SCD and JCNC significantly. The G-JCNC is known as exploiting the full channel gain from the observations. Also, separate channel decoding (SCD) outperforms the JCNC approach by around 2.5dB. Here fading channels are assumed, which result in possible combination at the equalizer output given (17) with different $\upsilon_{\mathrm{S,A}} \neq \upsilon_{\mathrm{S,B}}$.

The performances difference of the decoding schemes regarding different receive window sizes is rather small. Thus, almost no performance degradation is obtained by choosing 1, 2, or 3 neighbors. In the higher signal to noise ratio (SNR) region the performance is limited by the interference power, but the equalizer treat these interference terms sufficiently for either 1,2 or 3 neighbors, so that overall no difference is distinguishable, besides the complexity is significantly reduced.

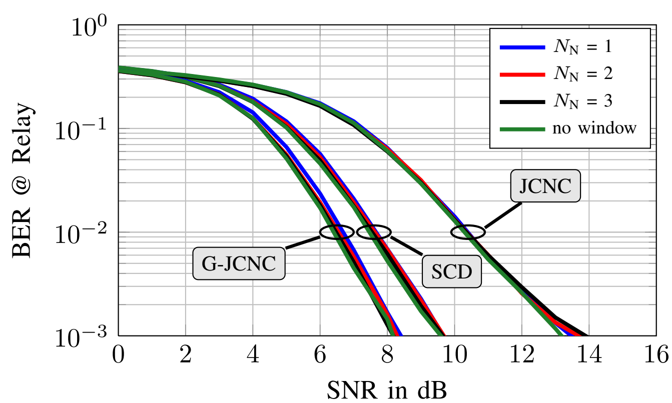

Fig. 7. BER performance at the relay of SCD, JCNC and G-JCNC using Gaussian transmit and receive filter, including the effect of delay and Doppler. $\tau_i<\tau_{\max}=0.08T$, $|\nu_i|<\nu_{\max}=0.08F$.

IV. CONCLUSION

In this paper, a first analyses on using Generalized FDM systems with Gaussian filters in a two way relay channel with physical-layer network coding was done. A linear equalizer which treats interference of the Gaussian transmit and receive filters was introduced and analyzed. The equalizer was simplified to consider a sufficient small number of adjacent symbols in the time-frequency grid. It was shown, that the output of the simplified equalizer is sufficient to calculate the a-posteriori probabilities, which are used in the detection/decoding process. Finally, a bit error rate performance evaluation was done and analyzed for three different detection/decoding schemes.

V. Acknowledgment

This work was supported in part by the German Research Foundation (DFG) under grant KU 1221/18-1 and WU 499/10-1 within the priority program “Communication in Interference Limited Networks (COIN)”, SPP 1397.

References

[1] F.-H.P. Fitzek, M. V. Pedersen, J. Heide, and M. Médard, “Network Coding: Applications and Implementations on Mobile Devices,” in *5th ACM Workshop on Performance Monitoring and Measurement of Heterogeneous Wireless and Wired Networks (PM2HW2N ’10)*, New York, NY, USA, 2010, ACM.

[2] R. Pabst, B. H. Walke, D.C. Schultz, P. Herhold, H. Yanikomeroglu, S. Mukherjee, H. Viswanathan, M. Lott, W. Zirwas, M. Dohler, H. Aghvami, D.D. Falconer, and G.P. Fettweis, “Relay-based Deployment Concepts for Wireless and Mobile Broadband Radio,” *IEEE Communications Magazine*, vol. 42, no. 9, pp. 80–89, Sept 2004.

[3] M. Dohler and Y. Li, *Cooperative Communications: Hardware, Channel & PHY*, Wiley, Chichester, U.K., 2010.

[4] J.N. Laneman, D.N.C. Tse, and G. W. Wornell, “Cooperative Diversity in Wireless Networks: Efficient Protocols and Outage Behavior,” *IEEE Transactions on Information Theory*, vol. 50, no. 12, pp. 3062–3080, Dec. 2004.

[5] S. Zhang, S.C. Liew, and P.P. Lam, “Hot Topic: Physical-layer Network Coding,” in *12th annual international conference on Mobile computing and networking (MobiCom 06)*, Los Angeles, CA, USA, 2006.

[6] S. Zhang, S.C. Liew, and P.P. Lam, “On the Synchronization of Physical-Layer Network Coding,” in *IEEE Information Theory Workshop (ITW ’06)*, Chengdu, China, Oct 2006, pp. 404–408.

[7] P. Popovski and H. Yomo, “Physical Network Coding in Two-Way Wireless Relay Channels,” in *IEEE International Conference on Communications (ICC’ 07)*, Glasgow, UK, June 2007.

[8] D. Wübben and Y. Lang, “Generalized Sum-Product Algorithm for Joint Channel Decoding and Physical-Layer Network Coding in Two-Way Relay Systems,” in *2010 IEEE Global Telecommunications Conference (GLOBECOM 2010)*, Miami, Fl, USA, Dec. 2010, IEEE.

[9] C. K. Ho, R. Zhang, and Y.-C. Liang, “Two-Way Relaying over OFDM: Optimized Tone Permutation and Power Allocation,” in *IEEE International Conference on Communications (ICC’ 08)*, Bejing, China, 2008.

[10] K. Jitvanichphaibool, Rui Zhang, and Ying-Chang Liang, “Optimal Resource Allocation for Two-Way Relay-Assisted OFDMA,” in *IEEE Global Telecommunications Conference (GLOBECOM 2008)*, New Orleans, LO, USA, Nov. 2008.

[11] D. Wübben, “Joint Channel Decoding and Physical-Layer Network Coding in Two-Way QPSK Relay Systems by a Generalized Sum-Product Algorithm,” in *7th International Symposium on Wireless Communication Systems (ISWCS 2010)*, York, UK, Sept. 2010.

[12] F. Li, G. Zhu, and D. Wang, “Optimal Power Allocation for Two-Way Relaying over OFDM using Physical-Layer Network Coding,” *The Journal of China Universities of Posts and Telecommunications*, vol. 18, no. 1, pp. 9–15, Feb. 2011.

[13] H. Shin and J. Lee, “Joint Resource Allocation for Multiuser Two-Way OFDMA Relay Networks with Proportional Fairness,” in *IEEE Vehicular Technology Conference (VTC Fall 2011)*, San Francisco, CA, USA, Sept. 2011.

[14] B. Han, W. Wang, and M. Peng, “Optimal Resource Allocation for Network Coding in Multiple Two-Way Relay OFDM Systems,” in *IEEE Wireless Communications and Networking Conference (WCNC 12)*, Paris, France, April 2012.

[15] D. Wübben, M. Wu, and A. Dekorsy, “Physical-Layer Network Coding with Multiple-Antenna Relays,” in *MIMO Processing for 4G and Beyond: Fundamentals and Evolution*. Apr 2014, CRC Press.

[16] M. Wu, F. Ludwig, M. Woltering, D. Wübben, A. Dekorsy, and S. Paul, “Analysis and Implementation for Physical-Layer Network Coding with Carrier Frequency Offset,” in *International ITG Workshop on Smart Antennas (WSA2014)*, Erlangen, Germany, Mar 2014.

[17] B. Farhang-Boroujeny, “OFDM Versus Filter Bank Multicarrier,” *IEEE Signal Processing Magazine*, vol. 28, no. 3, pp. 92–112, May 2011.

[18] V. Vakilian, T. Wild, F. Schaich, and S. ten Brink, “Universal-Filtered Multi-Carrier Technique for Wireless Systems Beyond LTE,” in *IEEE Global Telecommunications Conference (GLOBECOM 2013)*, Atlanta, GA, USA, Dec. 2013.

[19] J. Du, *"Pulse Shape Adaptation and Channel Estimation in Generalised Frequency Division Multiplexing Systems"*, Licentiate thesis in electronics and computer systems, KTH, Stockholm, Sweden, Nov. 2008.

[20] G. Fettweis, M. Krondorf, and S. Bittner, “GFDM - Generalized Frequency Division Multiplexing,” in *IEEE 69th Vehicular Technology Conference, (VTC Spring 2009)*, Barcelona, Spain, April 2009.

[21] G. Wunder, P. Jung, M. Kasparick, T. Wild, F. Schaich, Y. Chen, S. ten Brink, I. Gaspar, N. Michailow, A. Festag, L. Mendes, N. Cassiau, D. Ktnas, M. Dryjanski, S. Pietrzyk, B. Eged, P. Vago, and F. Wiedmann, “5GNOW: Non-Orthogonal, Asynchronous Waveforms for Future Mobile Applications,” *IEEE Communications Magazine*, vol. 52, no. 2, Feb. 2014.

[22] A. Sahin, I. Guvenc, and H. Arslan, “A Survey on Multicarrier Communications: Prototype Filters, Lattice Structures, and Implementation Aspects,” *IEEE Communications Surveys Tutorials*, vol. 16, no. 3, pp. 1312–1338, Mar. 2014.

[23] S. Schedler, M. Woltering, D. Wübben, V. Kühn, and A. Dekorsy, “Investigation on Gaussian Waveforms to Improve Robustness in Physical Layer Network Coding,” in *18th International OFDM Workshop 2014 (InOWo’14)*, Essen, Germany, Aug. 2014.

[24] K. Matheus, K. Knoche, M. Feuersanger, and K. D Kammeyer, “Two-dimensional (recursive) Channel Equalization for Multicarrier Systems with Soft Impulse Shaping (MCSIS),” in *Global Telecommunications Conference (GLOBECOM 1998)*, Dec. 1998, vol. 2.

[25] U. Bhat and T.M. Duman, “Decoding Strategies for Physical-Layer Network Coding over Frequency Selective Channels,” in *Wireless Communications and Networking Conference (WCNC), 2012 IEEE*, Paris, France, April 2012.

[26] M. Wu, D. Wübben, and A. Dekorsy, “Mutual Information Based Analysis for Physical-Layer Network Coding with Optimal Phase Control,” in *9th International ITG Conference on Systems, Communications and Coding (SCC’ 13)*, Munich, Germany, Jan. 2013.